Tellus (1983), *35A*, 73–80

A time dependent, two-layer frontal model of buoyant plume dynamics

By JAMES O'DONNELL and RICHARD W. GARVINE *College of Marine Studies, University of Delaware, Robinson Hall, Newark, DE 19711, U.S.A.*

(Manuscript received November 2, 1981; in final form March 16, 1982)

ABSTRACT

The dynamics of buoyant plumes, such as those observed at the mouths of the Mississippi and Connecticut Rivers is investigated by considering the one-dimensional, time dependent behavior of a two-layer, frontal model. The equations governing the flow in the main body of the plume are the long wave equations. The flow at the frontal boundary is modeled using jump conditions which incorporate the important dissipative processes. These equations are solved numerically using a shock patching technique that is accurate to second order in the long wave region and to first order at the front. The solutions demonstrate the controlling influence of the inlet on the flow field and the importance of time-dependent processes for the dynamics of buoyant plumes.

1. Introduction

Coastal circulation patterns at the mouths of major rivers are often dominated by the flow of a shallow layer of buoyant river water. These layers, often called plumes, have been observed at the mouths of the Connecticut (Garvine, 1974a), Mississippi (Wright and Coleman, 1971), Fraser (Stronach, 1981), and Great Whale (Ingram, 1981) rivers. Dynamically similar plumes are often formed by the discharge cooling water from power plants (Scarpace and Green, 1973).

Garvine (1982) reviews and summarizes the important observations and modeling attempts for these plumes and presents a novel, horizontally two-dimensional, steady state model of his own. This paper presents the one-dimensional, time dependent counterpart to that study. The principal objectives are to investigate the fundamental physical processes contained in the model and to develop and test the numerical scheme employed to solve the model equations. This information will be essential to the development of the solution to the full horizontally two-dimensional, time dependent problem of buoyant plume dynamics.

2. Model development

The conceptual basis for the model of the near field is the same as that used by Garvine (1982) and similar to that of Abbott (1961). The upper layer has two distinct domains. The first is the plume body, where the motion is inviscid and any turbulent interfacial mixing is negligible due to the high degree of stratification. The second domain, the frontal zone, is a small scale, highly dissipative region where turbulent exchange with the underlying ambient water results in both friction and mass entrainment, with the consequent dissipation of energy. Since the horizontal size of the frontal zone is very small compared to the plume body, it is treated as a discontinuity.

The mathematics describing the flow in the plume body can be developed using the coordinate system in Fig. 1. The system is earth fixed, and defined so that the plume propagates in the positive direction. The problem is restricted to cases where Coriolis effects can be neglected and where there are no gradients of flow variables in the y-direction. The symbol $D(x,t)$ denotes the local depth of the interface, which is regarded as small

0280-6495/83/010073-08$2.50/0

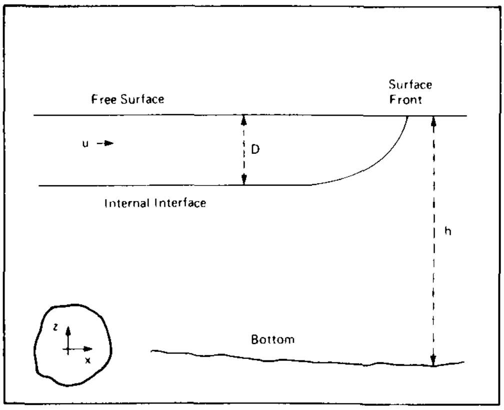

Fig. 1. Coordinate system for model.

compared to the total depth of the water column, h, throughout the space domain. The ambient water has a uniform density, ρ_a and the buoyant water is taken for simplicity to have a uniform density of $\rho_a - \Delta\rho$, where $\Delta\rho > 0$. $u(x,t)$ is the horizontal velocity of the fluid. The vertical momentum balance is assumed to be hydrostatic. Since $\Delta\rho/\rho_a$ is small for all plumes of interest, the Boussinesq approximation will be used. These assumptions allow the simplification that the pressure field is in isostatic equilibrium, and so the motion in the lower layer is essentially unaffected by the upper layer (Garvine, 1974b). For reasons of simplicity, the ambient fluid is further assumed to be stationary.

Using these restrictions and assumptions, the vertically integrated continuity and momentum equations governing the motion in the plume body are simply

$$D_t + (Du)_x = 0 \tag{1}$$

$$u_t + (uu_x) + g' D_x = 0 \tag{2}$$

Here x and t-subscripts imply derivatives.

These equations are mathematically identical to the nonlinear shallow water wave equations and to the compressible gas flow equations. They are thus hyperbolic, have real characteristics (Stoker, 1957, p. 291), and allow discontinuities in flow variables to propagate along these characteristics without smoothing.

These discontinuities must be treated as internal boundaries and therefore require special boundary, or jump, conditions. In compressible gas dynamics these discontinuities are called shocks and the boundary conditions are given by the Rankine–Hugoniot equations (Courant and Fredrichs, 1976). In hydraulics the discontinuities are called bores or jumps, and the appropriate jump conditions, for a single layer fluid, were derived by Stoker (1957).

Garvine (1981) derived frontal jump conditions for models of two-layer flows with discontinuities termed bores, shocks, jumps, seiches or surges, at which dissipation of energy takes place. These algebraic relations were derived by integration of the equations of mass and momentum across the discontinuity within which friction and entrainment were parameterized.

The jump conditions applied to buoyant surface plumes can be written as

$$u_1 = A u_f \tag{3}$$

$$c_1 = F_f^{-1} u_f \tag{4}$$

where u_1 is the fluid velocity behind the front, $c_1 = \sqrt{g' D_1}$ is the phase speed of a long, linear wave on the interface of depth D_1, the depth behind the front, and u_f is the frontal propagation velocity. F_f^{-1} and A are constants that depend on the dissipative processes at the front. Particular values selected were $A = 1.3$ and $F_f = 1.2$, the same as those used by Garvine (1981).

3. Numerical solution techniques

In keeping with the modeling philosophy, the numerical scheme treats the near field as two distinct regions. The flow in the inviscid region, or plume body, is calculated by the original method of Lax and Wendroff (1960), and the flow at the front is determined from the appropriate jump conditions using a shock fitting or patching technique, similar to Gary (1962).

The difference scheme described by Lax and Wendroff requires that eqs. (1) and (2) be written in conservation law form. After defining a new variable, the volume transport $m = Du$, (1) and (2) can be rewritten as,

$$\mathbf{W}_t + \mathbf{G}(\mathbf{W})_x = \mathbf{0} \tag{5}$$

where $\mathbf{G}(\mathbf{W})$ and $(\mathbf{W})$ are matrices defined as

$$\mathbf{W} \equiv \begin{Bmatrix} D \\ m \end{Bmatrix} \qquad \mathbf{G} \equiv \begin{Bmatrix} m \\ m^2/D + g' D^2/2 \end{Bmatrix}$$

and the subscripts t and x imply differentiation with respect to that variable. Eq. (5) can be written equivalently as

$$\mathbf{W}_t + \mathbf{A} \cdot \mathbf{W}_x = \mathbf{0}$$

where the matrix $\mathbf{A}$ is the Jacobian of $\mathbf{G(W)}$ with respect to $\mathbf{W}$, which for this problem is

$$\mathbf{A} \equiv \begin{Bmatrix} 0 & 1 \\ g' D - m^2/D & 2m/D \end{Bmatrix}$$

Using these matrices, the Lax and Wendroff difference scheme, equivalent to (1) and (2), appears as,

$$\mathbf{W}_{i,j+1} = \mathbf{W}_{i,j} - \left(\frac{\Delta t}{2\Delta x}\right) \{\mathbf{G}_{i+1,j} - \mathbf{G}_{i-1,j}\} + \frac{1}{2}\left(\frac{\Delta t}{\Delta x}\right)^2 \{\mathbf{A}^+(\mathbf{G}_{i+1,j} - \mathbf{G}_{i,j}) - \mathbf{A}^-(\mathbf{G}_{i,j} - \mathbf{G}_{i-1,j})\} \quad (6)$$

where, $x = i\Delta x$ and $t = j\Delta t$. The increments Δt and Δx define the separation of the grid points and $\mathbf{A}^+$ and $\mathbf{A}^-$ are calculated from

$$\mathbf{A}^+ = (\mathbf{A}_{i+1,j} + \mathbf{A}_{i,j})/2$$

and

$$\mathbf{A}^- = (\mathbf{A}_{i,j} + \mathbf{A}_{i-1,j})/2$$

It has been shown by Lax and Wendroff (1960) that eq. (6) is accurate to second order and that the stability of the scheme is assured if Δt and Δx satisfy the Courant–Friedrichs–Lewy condition, i.e., if

$$N_c \equiv (|u|_{\max} + c_{\max}) < 1$$

where $|u|_{\max}$ and $c_{\max}$ are the maximum values of $|u|$ and c, fluid velocity and interfacial wave phase velocity, in the domain of the problem. This condition is implemented by calculating Δt at each time step after specifying the Courant Number, N_c and Δx. This numerical procedure has been used successfully by several investigators for similar problems (Houghton, 1969; Houghton and Kasahara, 1968; Simons, 1978).

Application of Garvine's (1981) jump conditions at the frontal boundary requires reformulation of eqs. (1) and (2) in terms of characteristics. Defining the variable $c(x,t) = \sqrt{g' D(x,t)}$, allows (1) and (2) to be rewritten

$$2c_t + 2uc_x + cu_x = 0$$

$$u_t + uu_x + 2cc_x = 0$$

These have the characteristics, $s = u \pm c$ (Courant and Friedrichs, 1976), where $s = \mathrm{d}x/\mathrm{d}t$ is the slope of the characteristic line in the x,t plane. Along these lines the dependent variables are related by the characteristic equations

$$u + 2c = K^+ \quad \text{for } s = u + c \quad (7)$$

$$u - 2c = K^- \quad \text{for } s = u - c \quad (8)$$

where K^+ or K^- is constant on any particular characteristic line.

Fig. 2 shows the characteristic plane in the neighborhood of the front. The circles represent the regular grid points used by the Lax and Wendroff method and the solid curve is the path of the front. At $t = j\Delta t$, the location of the front is x_f^j, point A in Fig. 2, and its velocity is u_f^j. Assuming the flow field behind the front is known, or has been calculated, then the jump conditions and the characteristic relations, eqs. (3), (4), (7) and (8), give u_f^{j+1} and x_f^{j+1}. Simple first order estimates are

$$x_f^{j+1} = x_f^j + \Delta t u_f^j \quad (9)$$

$$u_f^{j+1} = (u_B + 2c_B)/(A + 2F_f^{-1}) \quad (10)$$

where u_B and c_B are the interpolated velocity and wave speed at B, the intersection of the $u + c$ characteristic which passes through x_f^{j+1}, and the

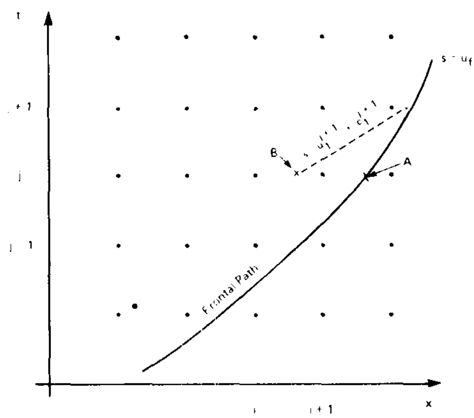

Fig. 2. Illustration of the numerical patching technique at the front.

line $t = j\Delta t$. The location of B is given to first order accuracy by

$$x_B = x_f^{j+1} - (u_1 + c_1)\Delta t \quad (11)$$

Since at each time step the flow at one, and sometimes two, grid points cannot be calculated using this method, values at such points were interpolated linearly between the last calculated grid point and the front. A more detailed description of this procedure is given by O'Donnell (1981).

The behavior of the Lax–Wendroff part of the scheme was tested by solving the same initial value problem as Houghton (1969), the formation of a hydraulic jump on the tropopause, and the full shock patching scheme was tested by solving the sudden release problem of Garvine (1981). Houghton's solutions were produced to within the resolution of his graphical presentation. Comparison of the numerical solution, after 400 time steps, to Garvine's analytic solution showed that the frontal velocities agreed to 0.1% and that any inaccuracies present in the rest of the flow field were too small to be detected in the plotted solution. These tests showed the scheme to be sufficiently accurate and stable. It was then used to perform the following numerical experiments.

4. Numerical experiments

These experiments were designed to examine the influence of the inlet conditions on the downstream flow, especially at the front, and to investigate in some detail the wave phenomena in the near field.

The length variable was normalized by the domain size, $\hat{x}$, which contained 1001 grid points, separated by $\Delta x = 10$ meters; thus, $\hat{x} = 10{,}000$ meters. The interfacial depth scale, $\hat{D}$, was chosen as D_p, the upstream limit of depth. The velocity scale was taken as $c_p = \sqrt{g' D_p}$. The time scale, $\hat{t}$, was defined as $\hat{t} = \hat{x}/c_p$. Hereafter all variables will be normalized using these three scales unless otherwise stated.

The initial conditions used in all experiments are prescribed as shown in Fig. 3. The depth and velocity behind the front are constant, and consistent with a frontal velocity of $u_f = 1.2$. Physically these conditions model what would occur if the buoyant spreading of a plume had been arrested, by a counterflowing current for example,

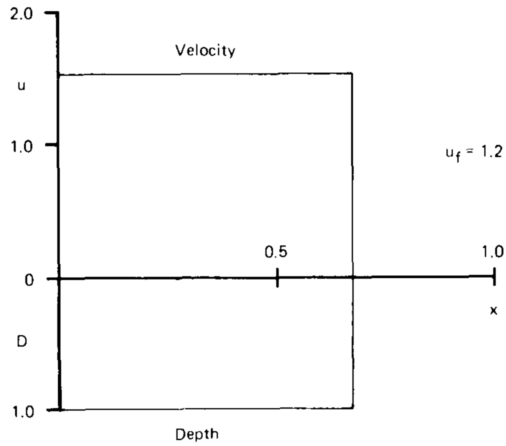

Fig. 3. Initial conditions used in numerical experiments.

and which then was instantaneously released and allowed to spread.

The boundary conditions at the front and at $x = 0$, the inlet, are more complicated to describe. At the front, the requirement that only one of the characteristic families intersects the front from upstream imposes certain constraints on the mixing parameters used in the jump conditions (O'Donnell, 1981). The values of A and F_f chosen ensure that the solution is properly determined at the front.

The boundary conditions at the inlet are constrained in a similar manner. If the u–c characteristics propagate upstream, i.e., in the negative x-direction, then u and c at the inlet, $x = 0$, defined as u_{in} and c_{in}, are not independent but have to satisfy the characteristic relations. Alternatively, if the characteristics propagate downstream, then both u_{in} and c_{in} must be specified. These two regimes can be distinguished by considering the slope of the u–c characteristic line at the inlet. The slope will be positive when the Froude number, $F_{in} \equiv u_{in}/c_{in}$, is greater than one (supercritical) and negative when $F_{in} < 1$ (subcritical). In the experiments described here, both u_{in} and c_{in} will be prescribed when $F_{in} > 1$. For cases with $F_{in} < 1$ the velocity, u_{in}, will be prescribed and the phase velocity, c_{in}, will be calculated in a manner analogous to the treatment of the flow at the frontal boundary.

In the first experiment, problem one, the inlet conditions are formulated to insure that the inlet flow is always supercritical, i.e., $F_{in} > 1$. This is accomplished by specifying the inlet transport, T, as a function of time and holding the Froude number constant. In order for the inlet and initial conditions to be compatible, $F_{in} = 1.56$. The depth and velocity at the inlet, D_{in} and u_{in} are then simply,

$$D_{in} = (T(t)/F_{in})^{2/3}, \qquad u_{in} = T(t)/D_{in}$$

where $T(t) \equiv m(x = 0, t)$ is the inlet transport as a function of time. This is specified as,

$$T(t) = \begin{Bmatrix} 1, & 0 \leqslant t < 0.1 \\ 1 + a(t - 0.1), & 0.1 \leqslant t < 0.2 \\ 1 + a(0.1), & 0.2 \leqslant t \end{Bmatrix}$$

This prescription simply changes the inlet transport linearly by an amount set by the factor, a, over a normalized time of 0.1.

Fig. 4 shows results for $a = -5$, corresponding to the reduction of the inlet transport by 50%.

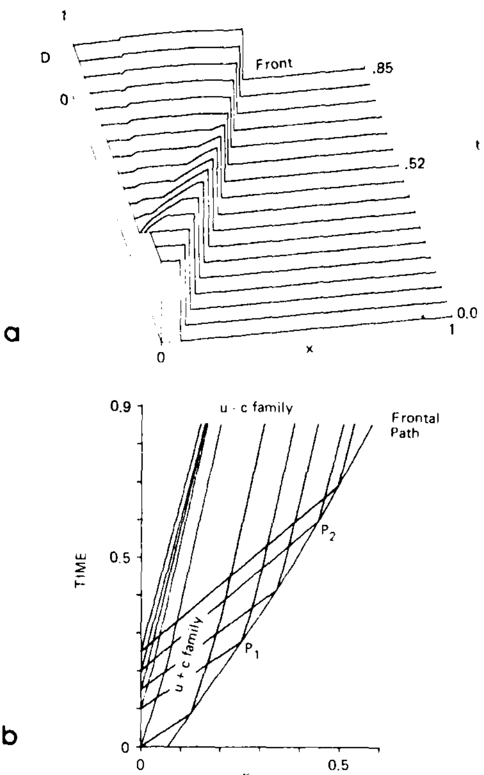

Fig. 4. Numerical solution to problem one: (a) shows the depth, D, as a function of x and t; (b) shows the corresponding characteristic diagram.

Fig. 4a shows a computer-generated three-dimensional projection of the interfacial depth, D, as a function of x and t. The important features of the flow are readily visible. There are two families of waves produced by the changing inlet conditions; since the flow is supercritical everywhere, both of these propagate to the right (positive x).

By analogy with compressible gas dynamics, the $u + c$ characteristics here are said to form a rarefaction wave family which can be clearly seen to overtake the front and then reduce the depth behind it. Close examination of the frontal path in Fig. 4b shows that the front is slowed by the rarefaction waves between the points labeled P_1 and P_2. These are the points of intersection of the frontal path and the characteristics bounding the rarefaction waves.

Fig. 4a also shows the development of a small internal hydraulic jump from a steepening wave in the region behind the expansion waves. This is the result of the convergence of the $u - c$ family of characteristics visible in Fig. 4b. This internal jump propagates with a velocity less than the frontal velocity, however, and so will never influence the flow field there.

The second problem shows the effect of rapidly increasing the inlet transport. This is similar to the compression wave problem of compressible gas dynamics where the interfacial depth here corresponds to the density in the gas. In this problem the inlet conditions have $a = 10$ and the initial conditions are modified slightly by having the initial frontal position at $x = 0.55$, but the flow behind is the same.

The development and steepening of the compression wave is clear in the depth field projection, Fig. 5a. This is caused by the convergence and intersection of the $u + c$ characteristics originating at the inlet during the changing flow conditions. These are shown in the characteristics diagram in Fig. 5b.

One of the basic assumptions used to formulate this model was that vertical entrainment in the plume body is negligible and that all dissipation occurs at the front. This was justified earlier; however, if internal surges and hydraulic jumps are an important part of the response, then their effects on the mass and momentum balances in the plume should be included in the model. This could be accomplished by patching the internal jump to the

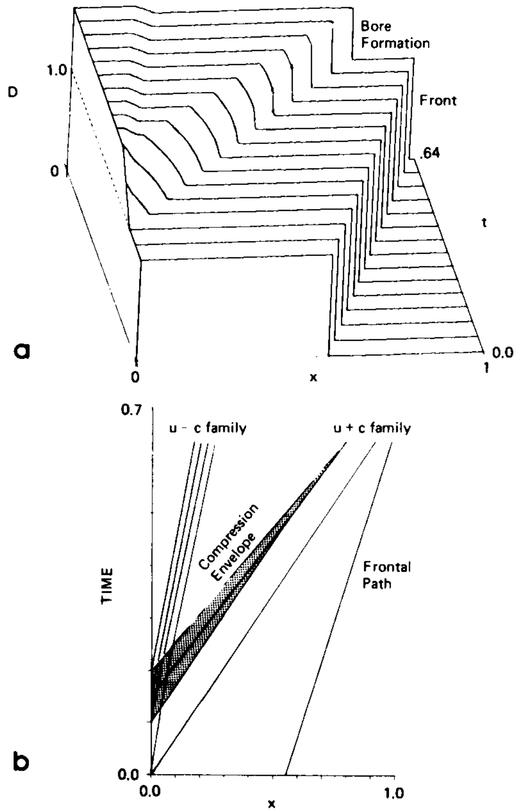

Fig. 5. Numerical solution to problem two: (a) shows the depth, D, as a function of x and t; (b) shows the corresponding characteristic diagram.

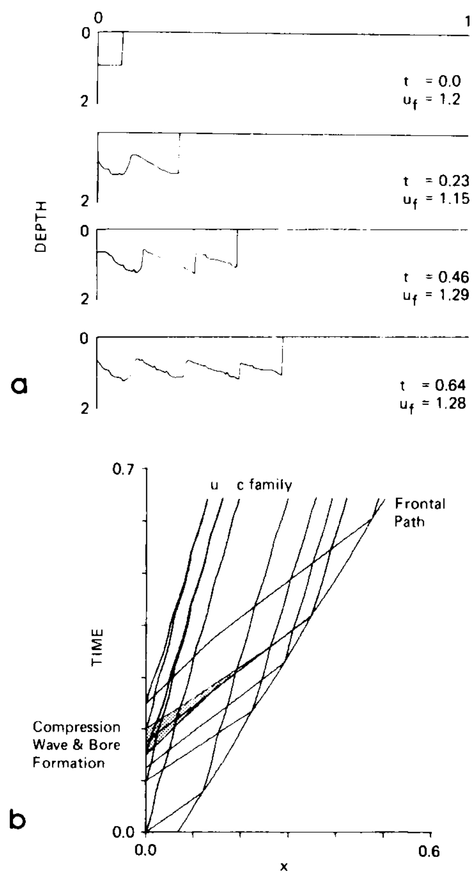

Fig. 6. Numerical solution to problem three: (a) shows depth, D, as a function of x at several values of t; (b) shows the characteristic diagram.

local flow using the appropriate jump conditions; however, this would require the use of more complicated algorithms and was not attempted.

Wiseman *et al.* (1976) reported time dependent phenomena that they interpreted as internal surges in the near field of the Mississippi River plume at South Pass. Although the evidence to support this interpretation was inconclusive, it is apparent that similar surges are valid solutions in the present model. Thus, a logical question is, what effect would such surges have on frontal motion?

Problem three attempts to answer this question. The initial conditions and the frontal boundary parameters are the same as for the first problem. The inlet conditions are set in the same manner with $F_{\text{In}} = 1.56$. Now, however, $T(t)$ is specified as a sinusoidal modulation about a given value T_0:

$$T(t) = T_0(1 + 0.5 \sin(20\pi t))$$

The solution is shown in Fig. 6. The modulated transport causes a series of compressions and rarefactions which later steepen and spread, respectively. The resulting depth field is shown in Fig. 6a. Here a three-dimensional projection was not practical, since certain large amplitude waves tend to obscure much of the rest of the field. Instead, a time sequence of depth versus x plots is shown. The path of the front, shown in the characteristic diagram, Fig. 6b, shows that when a surge overtakes the front, the sudden increase in depth and velocity that occurs causes the front to accelerate. The subsequent arrival of rarefaction waves then slowly decelerates the front until the next surge arrives. This causes a "scalloped" shape in the frontal path.

Several authors have suggested that the Froude number at the mouth of a highly stratified river or estuary which is in a steady state should be equal to, or slightly less than, unity (Stommel and Farmer, 1952; Wright and Coleman, 1971). Problem four demonstrates the behavior of the model when the inlet conditions become slightly subcritical. The previous initial and frontal conditions apply, but the inlet conditions must now be specified in a different way, as described above. For this case it proved convenient to specify the velocity, u_{in}, as a function of time and to keep c_{in} constant with $F_{in} < 1$, in which case c_{in} was calculated by the method described above. For this problem

$$u_{in}(t) = \begin{cases} 1.56, & 0.0 \leqslant t \leqslant 0.01 \\ 1.56\,(1 - a(t - 0.01)), & 0.01 < t \leqslant 0.11 \\ .156\,a, & 0.11 < t \end{cases}$$

where $a = 5.0$.

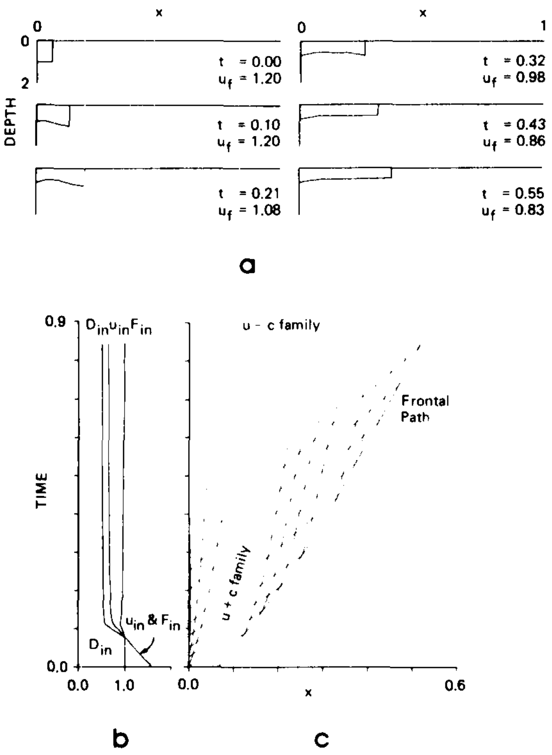

Fig. 7. Numerical solution to problem four: (a) shows the depth as a function of x at several values of t; (b) shows the time variation of u_{in}, F_{in}, and D_{in}; (c) is the characteristic diagram.

The results are shown in Fig. 7. The depth field, Fig. 7a, displays another simple rarefaction wave which slows the front. Fig. 7c shows the characteristics of the solution. Note that one of the u–c lines generated at $x = 0$, the inlet, changes direction and curves back to intersect the time axis. This demonstrates how the inlet conditions are partially controlled by the upstream flow. Fig. 7b shows a plot of the inlet variables as a function of time. Initially the velocity, u_{in}, and the Froude number, F_{in}, are identical until at $t = 0.08$ the inlet flow becomes subcritical and u_{in} and c_{in} vary independently. This occurs when the three lines shown in Fig. 7b intersect. An interesting aspect of the solution is the slight decrease that occurs in the phase speed c_{in} when the velocity u_{in} is held constant, at $t = 0.11$. This is apparent in Fig. 7b as the slight increase in F_{in}. No simple explanation is apparent, but it appears that the inlet flow is tending towards the critical state that Stommel and Farmer (1952) suggested for the steady state.

5. Summary and conclusions

In this paper, a model of buoyant plume dynamics has been developed in which the buoyant upper layer is divided into two domains, an inviscid zone, where there is no interfacial mixing and the buoyant spreading of the upper layer dominates, and a frontal zone where turbulent entrainment and friction are important. This model, which is the one-dimensional, time dependent counterpart to that of Garvine (1982), allows the plume to be described by comparatively simple mathematics. The governing equations are solved numerically with several different boundary conditions in order to illustrate some of the properties of the model.

The numerical scheme developed to solve the governing equations used the original Lax and Wendroff (1960) method in the inviscid zone and a first order shock patching technique at the front (O'Donnell, 1981). This procedure provided solutions which were both accurate and stable.

Since the present model is horizontally one-dimensional, direct comparison with buoyant plumes in nature is not possible, because they are nearly always strongly two-dimensional in the horizontal, as well as time dependent. Nevertheless, many of the fundamentals of plume dynamics can be understood by focusing, as here, on the time dependent behavior.

The results of the four numerical experiments decribed demonstrate that the frontal motion of buoyant plumes is strongly controlled by the flow at the inlet. Control is exerted by the generation of internal waves which propagate towards the front where they modify the flow. If changes in the inlet flow occur with short time scales, then these internal waves can develop into surges or bores which would effectively increase the amount of interfacial mixing. These results, together with those of Garvine (1982), encourage the extension of this model and its numerical solution technique, to two horizontal dimensions in order to more closely approximate the behavior of natural buoyant plumes.

6. Acknowledgement

The authors express their gratitude for support of this study by the National Science Foundation under Grant No. OCE-7821318.

REFERENCES

Abbott, M. B. 1961. On the spreading of one fluid over another. *La Houille Blanche*, 622–628 and 827–846.

Courant, R. and Friedrichs, K. O. 1976. *Supersonic flow and shock waves*. Interscience Publishers, Inc. New York, N.Y.

Garvine, R. W. 1974a. Physical features of the Connecticut River outflow during high discharge. *J. Geophys. Res. 79*, 831–846.

Garvine, R. W. 1974b. Dynamics of small scale oceanic fronts. *J. Phys. Oceanogr. 4*, 557–569.

Garvine, R. W. 1981. Frontal jump conditions for models of shallow buoyant surface layer hydrodynamics. *Tellus 33*, 301–312.

Garvine, R. W. 1982. A steady state model for buoyant surface plume hydrodynamics in coastal waters. *Tellus 34*, 293–306.

Gary, J. 1962. Numerical computation of hydrodynamic flows which contain a shock. Report NYO 9603, Courant Inst. Math. Sci., New York University.

Houghton, D. D. 1969. Effects of rotation on the formation of hydraulic jumps. *J. Geophys. Res. 74*, 1351–1360.

Houghton, D. D. and Kasahara, A. 1968. Nonlinear shallow fluid flow over an isolated ridge. *Comm. Pure Appl. Math. 13*, 1–23.

Ingram, R. G. 1981. Characteristics of the Great Whale River plume. *J. Geophys. Res. 86*, 2017–2023.

Lax, P. and Wendroff, B. (1960). Systems of conservation laws. *Comm. Pure Appl. Math. 13*, 216–237.

O'Donnell, J. 1981. Buoyant plumes: a numerical model. M.S. Thesis, College of Marine Studies, Univ. of Delaware, Newark, DE.

Scarpace, F. L. and Green III, T. 1973. Dynamic surface temperature structure of thermal plumes. *Water Resources Res. 9*, 138–153.

Simons, T. J. 1978. Generation and propagatioin of downwelling fronts. *J. Phys. Oceanogr. 8*, 571–581.

Stoker, J. J. 1957. *Water waves*. Interscience Publishers, New York, N.Y.

Stommel, H. and Farmer, H. G. 1952. Abrupt change in width in two-layer open channel flow. *J. Mar. Res. 11*, 205–214.

Stronach, J. A. 1981. The Fraser River plume, Strait of Georgia. *Ocean Management 6*, 201–221.

Wiseman, W. J., Wright, L. D., Rouse, L. J. and Coleman, J. M. 1976. Periodic phenomena at the mouth of the Mississippi River. *Contrib. Mar. Sci. 20*, 11–32.

Wright, L. D. and Coleman, J. M. 1971. Effluent expansion and interfacial mixing in the presence of a salt wedge, Mississippi River Delta. *J. Geophys. Res. 76*, 8849–8661.